Differentiation between Cellularized and Decellularized Mouse Kidneys using Mean Scatterer Spacing: A Preliminary Study*

Remie Nasr, *Member, IEEE*, Omar Falou, *Member, IEEE*, Eno Hysi, Lauren Wirtzfeld, Elizabeth S.L. Berndl and Michael C. Kolios, *Member, IEEE*

Abstract— **Scattering from the extracellular matrix (ECM) is currently being investigated, using a decellularization technique, which involves removing cells from tissue while preserving the ECM. This work aims to investigate the use of the mean scatterer spacing, using cepstral analysis techniques, for the differentiation between cellularized and decellularized mouse kidneys. After decellularization, the mean scatterer spacing decreased, with an average spacing for all the kidneys of 5.97 ± 1.89 µm before decellularization, and 5.38 ± 1.72 µm after decellularization. A significant difference was found between the calculated spacings from the kidneys, before and after decellularization. Future work include the incorporation of other parameters to further improve the sensitivity of this technique.**

I. Introduction

Three-dimensional scaffolds are commonly used in the field of tissue engineering. While new synthetic structures are being developed, there is still a great interest in exploring the extracellular matrix (ECM) of native tissues. A recently developed technique, known as "decellularization", allows for the removal of cells from intact tissue while preserving the ECM structure [1].

The extracellular matrix consists of proteins and other biomolecules synthesized by cells that, combined, make up each tissue [2]. The functionality of the tissue is defined by the composition and the architecture of the ECM, which is unique for each tissue. However, the composition and structure of each specific ECM protein is conserved among species [3], [4], making the ECM identifiable within and between species and largely without immune rejection. ECM scaffolds can serve as a powerful source to promote the formation of site-appropriate tissue at the site of implantation after injury, as long as they are properly processed to remove cellular antigens that would induce immune rejection. This has to be done without damaging the ECM [5].

The ECM obtained from decellularized tissue is used in regenerative medicine and tissue engineering strategies, with recent applications including the use of three-dimensional ECM scaffolds prepared by organ decellularization [6]–[10]. The goal of the decellularization technique is to remove all the cellular and nuclear materials efficiently while minimizing any unfavorable effect on the composition, biological activity, and mechanical integrity of the remaining ECM. The efficiency of cell removal from a tissue is dependent on the origin of the tissue and the methods used, which are presented in [11]. Each of these treatments affect the composition, tissue ultrastructure, and mechanical behavior of the remaining ECM scaffold, which in turn, affect the host response to the material [1].

High frequency ultrasound can be used for the characterization of tissue structures non-invasively, longitudinally, and without the need for tissue staining [12]. The ability to study the ultrasound backscatter from extracellular matrices offers new opportunities for characterizing the structure, such as estimating the mean scatterer spacing from the ECM. Cepstral analysis has been used to estimate the mean scatterer spacing [13], [14], for the characterization of chronic liver disease [15] and for liver-tissue characterization [16]. In this work, we investigate the use of cepstral analysis to estimate the mean scatterer spacing from ultrasound signals of mouse kidneys, before and after decellularization.

II. Materials and Methods

A. Cepstral Analysis

Quantitative cepstral techniques provide a method to reduce system effects in the spectrum of the received backscattered signal. The log operation in the cepstral technique converts the multiplicative relationship between the scatterer function and the system response in the Fourier domain to an additive one.

The power cepstrum of a signal, $C_p(n)$, is defined as the inverse Fourier transform of the logarithm of the power spectrum of the signal:

* This research has been supported by the Terry Fox Foundation, Canadian Institutes of Health Research (CIHR), and Canadian Breast Cancer Foundation (CBCF).

R. Nasr is with the Doctoral School of Science and Technology, Lebanese University, Tripoli, Lebanon (e-mail: remie.nasr@gmail.com).

O. Falou is with the Doctoral School of Science and Technology, Lebanese University, Tripoli, Lebanon; also with the Department of Science, American University of Culture and Education, Koura, Lebanon (e-mail: ofalou@gmail.com).

E. Hysi is with the Department of Physics, Ryerson University, Toronto, ON, Canada (e-mail: eno.hysi@gmail.com).

L. Wirtzfeld is with the Department of Physics, Ryerson University, Toronto, ON, Canada (e-mail: lauren.wirtzfeld@ryerson.ca).

E. Berndl is with the Department of Physics, Ryerson University, Toronto, ON, Canada (e-mail: eberndl@ryerson.ca).

M. C. Kolios is with the Department of Physics, Ryerson University, Toronto, ON, Canada (e-mail: mkolios@ryerson.ca).

978-1-5090-2555-8/16/$31.00 ©2016 IEEE

$$C_p(n) = IFT\{Log(|X(w)|^2)\} \quad (1)$$

where $X(w) = FT\{x(n)\}$, *FT* is the Fourier Transform, *IFT* is the Inverse Fourier Transform, and *x(n)* is the signal for which the cepstrum is applied [14].

B. Organs Preparation

Removing cells will alter the native three-dimensional architecture of the ECM. The most commonly utilized methods for decellularization of tissues involve a combination of physical and chemical treatments. The physical treatments can include agitation, mechanical massage or pressure, or freezing and thawing [17]. These methods disrupt the cell membrane, release cell contents, and facilitate subsequent rinsing and removal of the cell contents from the ECM.

In this work, a total of four kidneys were decellularized by washing the tissue in sodium dodecyl sulfate (SDS) for 24 hours, followed by washing with Triton-X for 24 hours and finally washing and storing in PBS. In this process, the ECM of the tissue is isolated from its native cells, leaving an ECM scaffold of the tissue.

C. Data Acquisition and Analysis

Kidneys were imaged after being maintained in PBS with a commercial high-frequency imaging system; the Vevo2100 (VisualSonics Inc, Toronto, ON) using nominal 40 MHz transducer. Then, after decellularization, the remaining extracellular matrix structures were re-imaged using the same machine settings.

From each kidney, ~130 imaging planes were acquired before and after decellularization. For each frame, a region of interest (ROI) was outlined on the reconstructed B-mode image. The ROI was chosen centered at the focus of the transducer and as large as possible as shown in Fig. 1.

Cepstral analysis was applied for each A-line from the chosen ROI. The obtained signal was then processed using Meyer wavelet for denoising, as shown in Fig. 2. The choice of the wavelet was based on the simulation done in previous work [18]. The improved performance after denoising is shown in Figs. 3a and 3b. It can be seen that, before applying wavelet denoising, the number of detected peaks is large; the spacing cannot be deduced since the same peak can be detected more than once. However, after applying the denoising technique, the peaks become prominent and the spacing can be easily detected. A threshold of 5% of the maximum peak value was then applied to remove the unwanted ripples.

Finally, the peaks were detected and the spacings between each two consecutive peaks were computed. The distance between each two consecutive peaks is equivalent to the value of the spacing, as reported in the literature [13]. After calculating the spacings from all tumor frames, the mean value was calculated for each kidney, before and after decellularization.

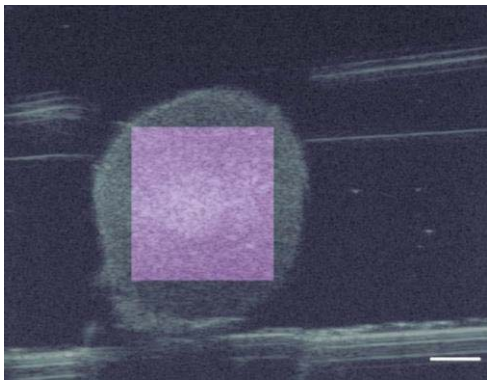

Fig. 1. Reconstructed B-mode image of one frame of a kidney. The square indicates the chosen ROI. The scale bar represents 1.5 mm.

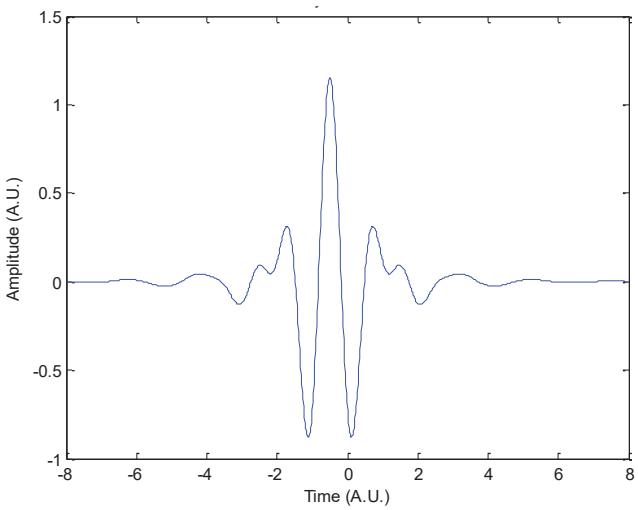

Fig. 2. Meyer Wavelet.

The Wilcoxon test of ranks was applied, where $p < 0.05$ is considered significant. Finally, the receiver operator characteristic (ROC) curve [19] was used to see if we could differentiate between cellularized and decellularized organs, using only one parameter: scatterer spacing. The area under the ROC curve (AUC) was calculated as a performance measure of this classifier in correctly classifying kidneys based on the mean scatterer spacing.

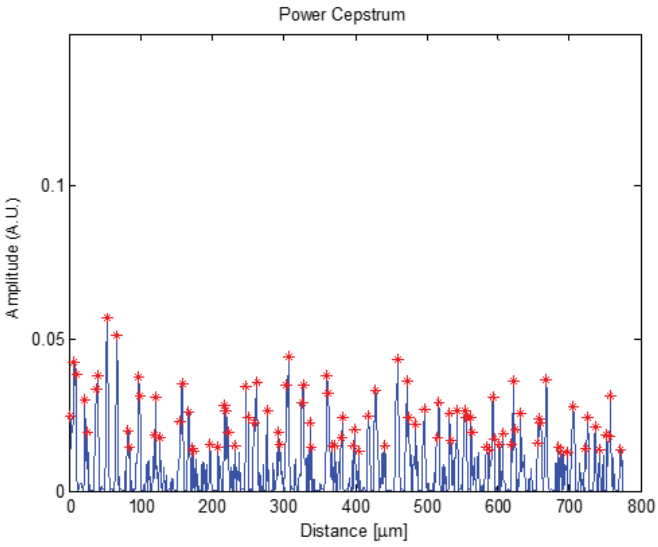

(a)

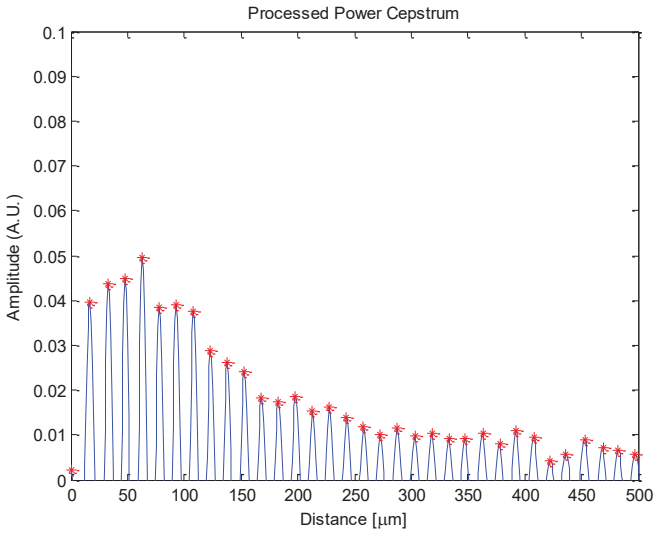

(b)

Fig. 3. The power cepstra of a single A-line from a simulated RF signal (a) before and (b) after wavelet denoising. The asterisks represent the detected peaks.

III. Results

The power cepstra for an individual A-line from a kidney and a decellularized kidney are shown in Figs. 4a and 4b, respectively.

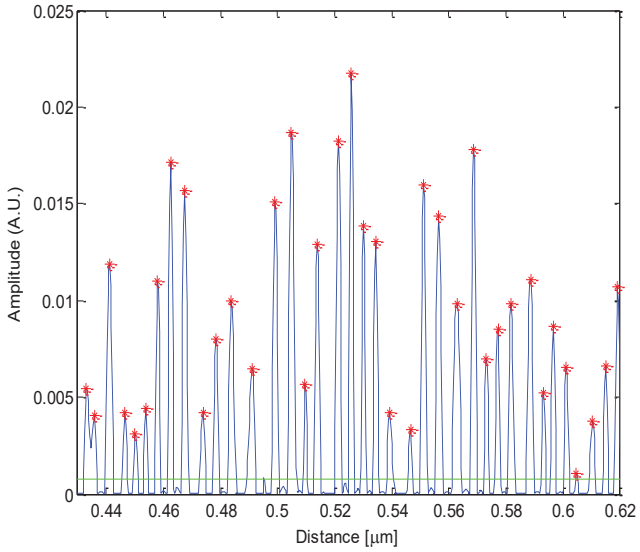

(a)

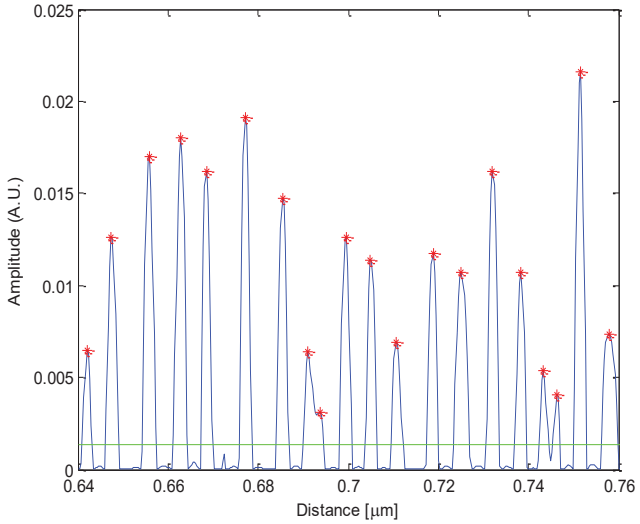

(b)

Fig. 4. The power cepstra of a single A-line from (a) cellularized and (b) decellularized kidneys. The horizontal line represents the threshold and the asterisks represent the detected peaks.

The values of the mean spacings between each two consecutive peaks for all the kidneys, before and after decellularization are shown in Table I.

TABLE I. Mean and Standard Deviation of the Spacing

	Cellularized			Decellularized		
	N (samples)	*Mean (μm)*	*SD (μm)*	*N (samples)*	*Mean (μm)*	*SD (μm)*
Kidney 1	726 600	5.47	1.73	235 700	5.09	1.58
Kidney 2	394 000	6.22	1.78	376 500	5.59	1.80
Kidney 3	669 500	6.30	2.02	368 100	5.13	1.66
Kidney 4	402 000	6.09	1.89	362 300	5.61	1.72
Average	2 192 100	5.97	1.90	1 342 600	5.38	1.72

When applying the Wilcoxon test of ranks, the p-value was found to be less than 0.01.

The values of the AUC obtained are presented in Table II.

TABLE II. AUC VALUES FOR EACH KIDNEY

	AUC
Kidney 1	0.57
Kidney 2	0.62
Kidney 3	0.68
Kidney 4	0.58

When combined together, a value of AUC for the average spacing for all kidneys was found to be 0.60. Fig. 5 shows the ROC curve for the combined kidneys.

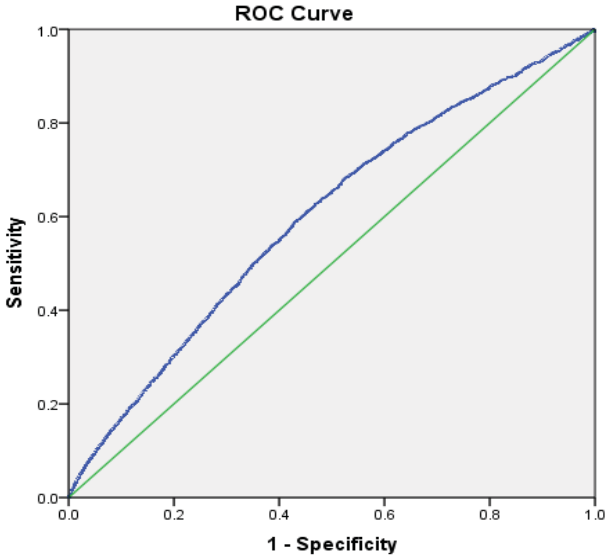

Fig. 5. ROC curve of all the kidneys.

IV. DISCUSSION

The goal of this work is to investigate the use of the mean scatterer spacing for the differentiation between cellularized and decellularized kidneys.

Kidneys have a well-known structure that appears to be semi-periodic. They are organized into small histologic units that are spaced apart by approximately the same distance. This may give rise to peaks which can be detected in the cepstrum since it is known that periodic components in the time domain signal manifest themselves as peaks in the cepstral domain; more precisely, at integer multiples of Δ, with Δ being the location of the dominant peak [20].

The mean spacing of the kidneys before decellularization is 5.97 ± 1.90 µm, while it is 5.38 ± 1.72 µm for the decellularized kidneys. The Wilcoxon test of ranks resulted in a p-value less than 0.05 which means that the scatterer spacings in both kidney groups, cellularized and decellularized, are significantly different. The ROC analysis was an attempt to determine whether it is possible to use the scatterer spacing to differentiate between these two groups. The area under the ROC curve is a reflection of how good the test is at distinguishing between two diagnostic groups. For each kidney, the values of the AUC were between 0.51 and 0.69 as shown in Table 2. The same results were obtained for all the kidneys combined, with an AUC of 0.60. In this range, the AUC is interpreted as a poor test and hence no discrimination between the two groups can be made. These findings are not surprising since after the decellularization, it is possible that the ECM did not undergo large structural changes, therefore the variation of the scatterer spacing was minimal. Instead of cells scattering the ultrasound pulse, equivalently sized fluid spheres (or the relevant fluid shapes) caused the scattering, which would result in relatively small changes in scattering. Moreover, the use of the scatterer spacing alone to classify cellularized and decellularized kidneys is not sufficient. Several quantitative ultrasound parameters, such as the midband fit, spectral slope and spectral intercept [21]–[24], can be combined individually with the mean scatterer spacing to find the best pairwise combination to improve the classification. Finally, denoising using wavelets will be investigated in order to optimize the choice of the wavelet while preserving the signal of interest.

V. CONCLUSION

The potential of using mean scatterer spacing to differentiate between kidneys, before and after decellularization was investigated. There is a clear difference between the values of the mean spacing before and after decellularization. However, the ROC analysis led to a relatively poor classification performance. Future work include choosing the appropriate wavelet for denoising and combining the scatterer spacing with other quantitative ultrasound parameters to improve the classification.

ACKNOWLEDGMENTS

The authors would like to acknowledge funding to support this work from Canada Foundation for Innovation, the Canada Research Chairs and The Terry Fox New Frontiers Program Project Grant in Ultrasound and MRI for Cancer Therapy (project #1034).

REFERENCES

[1] T. W. Gilbert, T. L. Sellaro, and S. F. Badylak, “Decellularization of tissues and organs.,” *Biomaterials*, vol. 27, no. 19, pp. 3675–83, Jul. 2006.

[2] C. M. Nelson and M. J. Bissell, “Of extracellular matrix, scaffolds, and signaling: tissue architecture regulates development, homeostasis, and cancer.,” *Annu. Rev. Cell Dev. Biol.*, vol. 22, pp. 287–309, Jan. 2006.

[3] M. P. Bernard, M. L. Chu, J. C. Myers, F. Ramirez, E. F. Eikenberry, and D. J. Prockop, “Nucleotide sequences of complementary deoxyribonucleic acids for the pro.alpha.1 chain of human type I procollagen. Statistical evaluation of structures that are conserved during evolution,” *Biochemistry*, vol. 22, no. 22, pp. 5213–5223, Oct. 1983.

[4] J. Exposito, M. D’Alessio, M. Solursh, and F. Ramirez, “Sea urchin collagen evolutionarily homologous to vertebrate pro-alpha 2(I) collagen,” *J. Biol. Chem.*, vol. 267, no. 22, pp. 15559–15562, Aug. 1992.

[5] S. F. Badylak, “The extracellular matrix as a biologic scaffold material.,” *Biomaterials*, vol. 28, no. 25, pp. 3587–93, Sep. 2007.

[6] D. A. Ott, H. C., Matthiesen, T. S., Goh, S., Black, L. D., Kren, S. M., Netoff, T. I., & Taylor, “Perfusion-decellularized matrix: using nature’s platform to engineer a bioartificial heart,” *Nature Medicine*, 2008. .

[7] B. E. Uygun, A. Soto-Gutierrez, H. Yagi, M.-L. Izamis, M. a Guzzardi, C. Shulman, J. Milwid, N. Kobayashi, A. Tilles, F. Berthiaume, M. Hertl, Y. Nahmias, M. L. Yarmush, and K. Uygun, "Organ reengineering through development of a transplantable recellularized liver graft using decellularized liver matrix.," *Nat. Med.*, vol. 16, no. 7, pp. 814–820, 2010.

[8] T. H. Petersen, E. A. Calle, L. Zhao, E. J. Lee, L. Gui, M. B. Raredon, K. Gavrilov, T. Yi, Z. W. Zhuang, C. Breuer, E. Herzog, and L. E. Niklason, "Tissue-engineered lungs for in vivo implantation.," *Science*, vol. 329, no. 5991, pp. 538–541, Jul. 2010.

[9] J. Cortiella, J. Niles, A. Cantu, A. Brettler, A. Pham, G. Vargas, S. Winston, J. Wang, S. Walls, and J. E. Nichols, "Influence of Acellular Natural Lung Matrix on Murine Embryonic Stem Cell Differentiation and Tissue Formation."

[10] J. M. Wainwright, C. A. Czajka, U. B. Patel, D. O. Freytes, K. Tobita, T. W. Gilbert, and S. F. Badylak, "Preparation of Cardiac Extracellular Matrix from an Intact Porcine Heart," *Tissue Eng. Part C Methods*, vol. 16, no. 3, pp. 525–532, 2010.

[11] P. M. Crapo, T. W. Gilbert, and S. F. Badylak, "An overview of tissue and whole organ decellularization processes.," *Biomaterials*, vol. 32, no. 12, pp. 3233–43, Apr. 2011.

[12] K. P. Hercado, M. Helguera, D. C. Hocking, and D. Dalecki, "Estimating Cell Concentration in Three-Dimensional Engineered Tissues Using High Frequency Quantitative Ultrasound," *Ann. Biomed. Eng.*, vol. 42, no. 6, pp. 1292–1304, 2014.

[13] K. a Wear, R. F. Wagner, M. F. Insana, and T. J. Hall, "Application of autoregressive spectral analysis to cepstral estimation of mean scatterer spacing.," *IEEE Trans. Ultrason. Ferroelectr. Freq. Control*, vol. 40, no. 1, pp. 50–58, 1993.

[14] R. S. Mia, M. H. Loew, K. a Wear, and R. F. Wagner, "Quantitative Estimation of Scatterer Spacing from Backscattered Ultrasound Signals Using the Complex Cepstrum," *Proc. 15th Int. Conf. Inf. Process. Med. Imaging. Springer-Verlag*, pp. 513–518, 1997.

[15] K. Suzuki, N. Hayashi, Y. Sasaki, M. Kono, Y. Imai, H. Fusamoto, and T. Kamada, "Ultrasonic tissue characterization of chronic liver disease using cepstral analysis.," *Gastroenterology*, vol. 101, no. 5, pp. 1325–1331, 1991.

[16] F. Lizzi, E. Feleppa, and N. Jaremko, "Liver-Tissue Characterization by Digital Spectrum and Cepstrum Analysis," *1981 Ultrason. Symp.*, 1981.

[17] T. W. Gilbert, "Strategies for tissue and organ decellularization," *J. Cell. Biochem.*, vol. 113, no. 7, pp. 2217–2222, 2012.

[18] R. Nasr, O. Falou, L. Wirtzfeld, E. Berndl, and M. Kolios, "Mean scatterer spacing estimation from pellets using cepstral analysis: A preliminary study," in *2015 International Conference on Advances in Biomedical Engineering (ICABME)*, 2015, pp. 305–308.

[19] J. A. Hanley and B. J. McNeil, "The meaning and use of the area under a receiver operating characteristic (ROC) curve.," *Radiology*, vol. 143, no. 1, pp. 29–36, Apr. 1982.

[20] T. Varghese and K. D. Donohue, "Mean-scatterer spacing estimates with spectral correlation.," *J. Acoust. Soc. Am.*, vol. 96, no. 6, pp. 3504–3515, 1994.

[21] A. Sadeghi-Naini, N. Papanicolau, O. Falou, J. Zubovits, R. Dent, S. Verma, M. E. Trudeau, J. F. Boileau, J. Spayne, S. Iradji, E. Sofroni, J. Lee, S. Lemon-Wong, M. J. Yaffe, M. C. Kolios, and G. J. Czarnota, "Quantitative Ultrasound Evaluation of Tumour Cell Death Response in Locally Advanced Breast Cancer Patients Receiving Chemotherapy.," *Clin. Cancer Res.*, vol. 19, no. 5, pp. 2163–2174, 2013.

[22] H. Tadayyon, A. Sadeghi-Naini, L. Wirtzfeld, F. C. Wright, and G. Czarnota, "Quantitative ultrasound characterization of locally advanced breast cancer by estimation of its scatterer properties.," *Med. Phys.*, vol. 41, no. 1, p. 012903, 2014.

[23] M. C. Kolios, G. J. Czarnota, M. Lee, J. W. Hunt, and M. D. Sherar, "Ultrasonic spectral parameter characterization of apoptosis," *Ultrasound Med. Biol.*, vol. 28, no. 5, pp. 589–597, 2002.

[24] L. A. Wirtzfeld, E. S. L. Berndl, and M. C. Kolios, "Ultrasonic Characterization of Extra-Cellular Matrix in Decellularized Murine Kidney and Liver," *2015 IEEE Int. Ultrason. Symp. Proc.*, pp. 3–6, 2015.